

Research Article

Ruminal CO₂ Holdup Monitoring: Acidosis Might Be Caused by CO₂ Poisoning

José Alberto Laporte-Urbe¹¹. Gemeinschaftskrankenhaus Herdecke, Herdecke, Germany

The ruminal buffering system composed of bicarbonate (HCO_3^-) and dissolved CO₂ (dCO_2) is indirectly related to the ruminal pH scale. While low pH generally indicates high dCO_2 formation, the pH scale is ratio and fail to provide individual component concentrations. For instance, modern feeding practices can reduce ruminal CO₂ gas effervescence from the ruminal fluid or "CO₂ holdup". Under those conditions, not only dCO_2 can reach critical concentrations, but the buffering system might favour HCO_3^- formation resulting in normal ruminal pH values, the quotient, regardless of the harmful dCO_2 accumulation. Consequently, subacute ruminal acidosis (SARA), traditionally associated with low or variable pH, might be triggered by CO₂ holdup. This study explores the application of an attenuated total reflectance infrared (ATR-IR) spectrometer for continuous dCO_2 monitoring and CO₂ holdup characterization. Three lactating dairy cattle were longitudinally exposed to diets designed to elevate both ruminal dCO_2 and SARA risk. Indwelling pH sensors and ruminal fluid samples served as references, while a categorical analysis detected CO₂ holdup from the output of the ATR-IR sensor. Milk yield, milk components, and feed intake supported the known positive role for high dCO_2 in rumen function. However, SARA was associated with ruminal CO₂ holdup, suggesting that prolonged exposure to critical dCO_2 concentrations during extended postprandial periods might trigger SARA. Continuous dCO_2 monitoring with the proposed methodology and analysis may offer a valuable tool for optimizing rumen function and prevent SARA risk.

Correspondence: papers@team.qeios.com — Qeios will forward to the authors

Introduction

According to Arrhenius' theory pH signals water (H_2O) ionisation into hydronium (H_3O^+) and hydroxides (HO^-) and their equilibrium. In the rumen, the pH scale indirectly measures the effect of bicarbonate (HCO_3^-) buffering and dCO_2 formation on H_3O^+ activity (Laporte-Urbe, 2016, 2019). In fact, the equilibrium between these two main molecules of the CO₂ buffer system causes ruminal pH fluctuations (Turner and Hodgetts,

1955). For instance, the ruminal short-chain fatty acid (SCFA) concentrations are seemingly constant (Dijkstra et al., 1993), are dominated by bases, $pK_a \sim 4.7$, and play only a buffering role when the pH is below 5.4 and the main CO_2 buffer system is depleted (Turner and Hodgetts, 1955; Hille et al., 2016). Moreover, the threshold for ruminal acidosis, pH 5.5 (Nocek et al., 2002), rumen fluid equilibrium pK_a' 6.1 (Hille et al., 2016) and the pH scale range, 5 to 7 (De Veth and Kolver, 2001), coincides with the CO_2 species equilibrium constants described by the Bjerrum equations (Buchholz et al., 2014). In fact, the relationship between SCFA formation and ruminal pH may simply be a consequence of CO_2 release during fermentation (Wolin, 1960; Dijkstra et al., 2012). Therefore, increased SCFA production leads to greater dCO_2 availability and lower ruminal pH.

The CO_2 buffer system works by combining protons, H_3O^+ , and HCO_3^- catalysed by the ruminal carbonic anhydrase to produce dCO_2 , the main liquid CO_2 form in the ruminal fluid, carbonic acid is short-lived in H_2O , <1% (Laporte-Urbe, 2016). The ruminal fluid is buffered, and H_2O dissociation reduced (pH increase), when dCO_2 dissociates into H_2O and CO_2 gas, which subsequently evolves into the ruminal gas cap to be released via eructation.

The ruminal HCO_3^- and dCO_2 concentrations are influenced by factors such as the diet, metabolism, and physicochemical characteristics of the rumen liquor (Hille et al., 2016; Laporte-Urbe, 2016, 2019). Conversely, ruminal dCO_2 and CO_2 blood pools rapidly equate (Whitelaw et al., 1972; Veenhuizen et al., 1988) due to the positive ruminal gradient with the blood, approximately 60 versus 2.5 mM (Turner and Hodgetts, 1955; Kohn and Dunlap, 1998) and the preferential use of ruminal CO_2 for SCFA uptake (Ash and Dobson, 1963; Rackwitz and Gabel, 2018).

The risk of subacute ruminal acidosis (SARA) is attributed to prolonged exposure to low ruminal pH (Nocek et al., 2002; AlZahal et al., 2007a; Villot et al., 2018), which might indicate high dCO_2 formation (Henderson-Hasselbalch equation, Eq 2). However, SARA individual risk is associated with variable pH bouts (Penner et al., 2007), suggesting increased HCO_3^- formation, and thus fluctuating pH (Eq 2). Moreover, modern feeding practices may reduce ruminal CO_2 effervescence (fugacity), leading to CO_2 holdup (Laporte-Urbe, 2016), which could explain dCO_2 accumulation and HCO_3^- formation. Consequently, the proposed timescale and risk for SARA onset might involve prolonged exposure to critical dCO_2 concentrations, resulting in CO_2 poisoning.

Ruminal dCO_2 concentrations are partially characterised (Chou and Walker, 1964b, a; Laporte-Urbe, 2019; Wang et al., 2019) and CO_2 holdup has never been observed *in situ*. In this study, I described the application and interpretation of a wired attenuated total reflectance infrared spectrometer (ATR-IR) designed to detect the distinctive IR signal of dCO_2 at $4.27 \mu m$ (Schädle et al., 2016) in the ruminal liquor. I hypothesised that the more

reliable ATR-IR technique and evaluation might (1) confirm the ruminal dCO₂ range, (2) unveil the relationship between dCO₂ and pH, and (3) disclose the role of CO₂ holdup on disease (SARA) and rumen function.

Materials and Methods

Ethical and experimental guidelines

The experimental protocols were approved and licensed by the Animal Care and Ethics Committee of Wageningen University and Livestock Research, WUR Dairy Campus, according to the Experiment in Animals Act, WOD, The Netherlands with permit AVD401002015298. The care of all cattle involved in this experiment adhered to the guidelines of the ethical committee for the use of fistulated cattle in tied stall facilities.

The experimental setup

The diets and cattle performance were described previously (Laporte-Urbe, 2019). In brief, 3 fistulated (Bar Diamond Inc., Ida., USA; 10 cm diameter) lactating dairy cattle, ~100 days in milk (DIM), were housed in tied stalls. The cattle were milked twice daily with ad libitum access to drinking water. Three total mixed ratio (TMR) diets were prepared daily using an automatic feeding system (Trioliet Feeding Technology, Oldenzaal, The Netherlands) and were served in equal parts, three times per day. The SARA-prone diets were a low physically effective neutral detergent fibre (Low-peNDF), a high ruminally degradable starch (High-RDS) and a combination of both (Combined); please see Laporte-Urbe (2019) for details on the formulation. All cattle were fed the same diet simultaneously for two weeks (run): the second week was for ruminal sampling and sensor deployment. The cattle had a three-days rest period between runs on a standard production TMR diet (Dairy Campus, Wageningen University). Indwelling pH sensors and manual ruminal samples were used as references.

Sensor deployment

The pH from the ventral ruminal sac was recorded every 15 sec for three days with indwelling pH sensors in all cattle (DASCOR, Inc., CA, USA). For continuously monitoring of the ruminal dCO₂ concentrations in one random sentinel cow per run, a wired ATR-IR sensor, VS-3000/3000E Sensor System (BevSense LLC, MA, USA, formerly VitalSensors Technologies LLC), was employed. The ATR-IR was placed into the ventral ruminal sac, and the dCO₂ was recorded every 10 sec for three days. The wire was exteriorised through the cannula, sealed to reduce CO₂ losses, and connected to the sensor Management Station, VS-300 (BevSense LLC, MA, USA).

All pH sensors were calibrated before and after placement using a three-point calibration protocol (DASCOR, Inc., CA, USA). The ATR-IR sensor came calibrated for sensing dCO₂ specific IR signal at 4.27 μ m in liquids ranging from 0 to 273 mM with a resolution of 0.02 mM, a repeatability of 0.36 mM and an accuracy of 0.89

mM; see the product specification for details (BevSense LLC, MA, USA, <https://www.beveragesensors.com>). Nevertheless, validation of the ruminal dCO₂ values and range was advised using a three-point alignment protocol developed for steady fermentative processes (Operative Manual, BevSense LLC, MA, USA). The following modified protocol was adopted due to the dynamic nature of the ruminal environment.

Ruminal fluid samples and calculations

The ventral ruminal sac fluid was manually sampled five consecutive times postprandially, 07:00h (0.5 h, 1 h, 2 h, 4 h, 6 h) during the first three days of the experimental week in all cattle. The pH of the samples was recorded with a temperature-corrected handheld system (Seven2Go ProS8, Mettler-Toledo). Approximately 30 ml of rumen fluid was alkalisied by the addition of 1 ml of 5 M sodium hydroxide (NaOH) solution and was frozen for subsequent TIC analysis (-20 °C). The goal was to retain TIC in HCO₃⁻ form by increasing the pH of the sample (pH ~10), according to the protocols given by the reference laboratory (Buchholz et al., 2014). TIC was determined by gas chromatography (GC) at the Institute of Biochemical Engineering, University of Stuttgart.

Calculations of CO₂ species. The ruminal dCO₂ concentrations were computed from the TIC using the Bjerrum plot equation (Eq. 1) and described as the **observed dCO₂**. The **calculated dCO₂** was derived from the TIC as if only HCO₃⁻ was recovered. The **calculated HCO₃⁻** was derived from the average pH and dCO₂ sensor reading for each min in a day (1,440 records). Both the **calculated dCO₂** and **calculated HCO₃⁻** were computed using the Henderson-Hasselbalch equation (Eq. 2).

$$dCO_2 = \frac{[H_3O^+]^2}{[H_3O^+]^2 + K_{a1} * [H_3O^+] + K_{a1} * K_{a2}} * TIC \quad (Eq. 1)$$

$$-\log[H_3O^+] = -\log K_{a1} + \log\left(\frac{HCO_3^-}{dCO_2}\right) \quad (Eq. 2)$$

where dCO₂ is the dissolved carbon dioxide (mM); HCO₃⁻ is bicarbonate (mM); TIC is the total inorganic carbon (mM); [H₃O⁺] is the hydrogen/hydronium activity derived from the pH of the sample (10^{-pH}); the 1st dissociation constant (K_{a1}) 4.45 × 10⁻⁷; and the 2nd dissociation constant (K_{a2}) 4.69 × 10⁻¹¹ at 25 °C.

Raw values from the ATR-IR sensor were expressed in parts per million per 100 g of H₂O (ppm/100 g H₂O) and the following formula was used to convert these values to millimole per litre (mM) of ruminal dCO₂.

$$x\left(\frac{ppm}{100gH_2O}\right) = y\left(\frac{mg}{100gH_2O}\right) \quad (Eq. 3.1)$$

and

$$z(mM) = \frac{y}{44.01 * 10} \quad (Eq. 3.2)$$

where x is the ruminal dCO_2 concentration in parts per million per 100 g of H_2O (ppm/100 g of H_2O) y is the dCO_2 in milligrams per one hundred grams of water (mg/100 g H_2O), and z is the dCO_2 in millimoles per litre (mM).

Analysis and statistics

All values from the dCO_2 and pH sensors were used in the development of the categorical analysis except for the records made one hour after deployment. A histogram method was used to detect outliers in the sensors' output (Gebiski and Wong, 2007). The pH sensors yielded no outliers, and ATR-IR yielded only few values. Values for CO_2 and HCO_3^- from the ruminal manual samples were compiled together. All descriptive statistical analyses and graphics were carried out in Origin 2020 (Origin Lab Corporation, MA, USA).

Categorical analysis to observe ruminal CO_2 holdup

The area under the curve for ruminal pH (AUC, pH units per min) emphasises the duration of the acidotic bouts at specific thresholds (Nocek et al., 2002). AlZahal et al. (2007a) employed the cumulative time under the curve to define a cut-off point for half-day exposure. More recently, Villot et al. (2018) normalised ruminal pH recordings and described two optimal thresholds, 30th and 50th percentile, for SARA detection. Previously, a “categorical analysis” was proposed to observe ruminal pH in the New Zealand pastoral system (Gibbs and Laporte Uribe, 2009). Our assumption was that changes in sensor location, due to the mixing movements and by the influx and outflow of nutrients led to the recording of distinct pH values. Nevertheless, with sufficient “iterations”, the pH category with the highest frequency was consistently identified, such as in several cattle, days, and short recording intervals (<15 seconds). The four categories for ruminal pH values were “Critical,” (pH <5.4), “Acidic” (pH between 5.4 and 5.8), “Optimal” (pH between 5.8 and 6.4), and “Suboptimal” (pH > 6.4), reflecting the state of the art on ruminal pH effect. For instance, cattle with pH values lower than 5.4 and 5.8 for 3 to 5 h/d have a high risk of ruminal acidosis and SARA (Dohme et al., 2008; Villot et al., 2018). Bacterial protein synthesis and fibre digestion diminish when the pH falls below 5.8, which is also recognised as a sign of ruminal dysfunction (Russell, 1998; De Veth and Kolver, 2001). Values around 6.4 are in the upper range in cattle given a TMR and are optimal for fermentation in pasture-based diets (Russell, 1998; De Veth and Kolver, 2001).

To my knowledge this is the first time that continuously recordings of ruminal dCO_2 have been performed, and thresholds for ruminal dCO_2 function remain undefined. However, CO_2 holdup can be identified by assigning a probability value derived from the normal cumulative distribution function (Eq. 4). Accordingly, four categories for ruminal dCO_2 were defined: “Low” for values below the 10th percentile, “Normal” for values between the

10th and 50th percentiles, "High" for values between the 50th and 90th percentiles, and "Critical" for values above the 90th percentile.

$$F(x) = \frac{1}{2} \left[1 + \operatorname{erf} \left(\frac{x - \mu}{\sigma \sqrt{2}} \right) \right] \quad (\text{Eq. 4})$$

where "x" is the recorded dCO₂ value, "μ" is the overall dCO₂ mean, and "σ" is the overall standard deviation for the experiment.

To comprehend the daily variation in these parameters and monitor CO₂ holdup, the day was divided into discrete segments of 10-min, e.g., 0:00, 0:10..., 23:50, or 144 segments. I chose this interval based on visual inspection, i.e., details were lost with longer intervals, and intervals smaller than 10-min might require shorter sampling frequencies or more iterations. Therefore, the "frequency" for each category was calculated by adding all the recorded values throughout the experiment for the 10-min interval. The AUC (%) for each category was the frequency divided by the total number of observations within that 10-min segment, multiplied by one hundred. The graphical representation, a 100% stacked area, provided a succinct overview of the calculated AUC for pH, Fig. 2.1a-c, and dCO₂, Fig. 2.2a-c.

Results and Discussion

Repeated acidosis challenges can lead to SARA (Dohme et al., 2008), and the diets were fed in subsequent two-weeks periods. Cattle during the first run on the Low-peNDF diet experienced increased milk yield, they developed SARA when fed the High-RDS diet in the second run and returned to a pre-trial performance when fed the Combine diet, third run (Laporte-Urbe, 2019). Accordingly, this report focuses on ruminal dCO₂ monitoring with the ATR-IR spectrometer and does not reiterate on these previously established facts which are again summarised in Table 2.

This is the first time that ATR-IR was used to monitor continuously in situ ruminal dCO₂ concentrations. It was uncertain whether ruminal dCO₂ would exceed ~60 mM (Kohn and Dunlap, 1998), whether CO₂ holdup would develop, or if the dietary treatments would produce signs of SARA. Early work revealed high and varied ruminal dCO₂ (Ash and Dobson, 1963; Chou and Walker, 1964b, a), but confirming its presence by manually sampling the rumen was challenging, Table 1 (Hille et al., 2016; Laporte-Urbe, 2019; Wang et al., 2019). The TIC sampling protocols adhered to the laboratory's recommendations (Buchholz et al., 2014), recognizing that freezing and transporting ruminal samples could lead to dCO₂ losses (Hille et al., 2016). However, this report relies instead on the more established and accurate ATR-IR technique targeting the specific IR signal of dCO₂ to confirm the ruminal dCO₂ range and presence (Schädle et al., 2016). Moreover, the widespread use of the ruminal pH scale (Nocek et al., 2002; AlZahal et al., 2007b) has obscured the well-established significance of dCO₂ in rumen

function (Ash and Dobson, 1963; Gabel et al., 1991). As you are about to observe, ruminal dCO_2 did exist in substantial quantities, and rather than solely attributing changes in rumen function to the diet or feeding sequence, we should also consider the role that these large variations in ruminal dCO_2 concentrations might elicit on the epithelium and bacterial activity.

Manual sampling versus continuous ruminal CO_2 monitoring. Table 1 summarises the values for pH, total inorganic carbon, TIC, and the **observed dCO_2** obtained by through manual sampling the ventral ruminal sac. I previously proposed that manual TIC sampling protocol used in these experiments primarily recovered ruminal HCO_3^- (Laporte-Urbe, 2019). For instance, the marked difference between manual (0.5 points higher) and continuous pH monitoring (Duffield et al., 2004; AlZahal et al., 2007b) is attributed to dCO_2 losses during manual sampling (Turner and Hodgetts, 1955; Kohn and Dunlap, 1998). To verify this assumption, **calculated HCO_3^-** was derived by averaging the continuous pH and dCO_2 measurements (Eq 2). The **calculated HCO_3^-** closely resembled the TIC values for all diets, which confirmed that mostly HCO_3^- was recovered via manual sampling. Subsequently, **calculated dCO_2** was computed from TIC (now HCO_3^-) and compared to the **continuous dCO_2** values derived from the ATR-IR sensor, as presented in Table 1 (Eq 1).

Discrete manual sampling and continuous measurement represent different techniques with distinct outcomes (Duffield et al., 2004; AlZahal et al., 2007b) are not readily comparable due to variations in time scales and sampling locations. Acidification of ruminal fluid samples in the past has yielded substantial TIC recovery (Chou and Walker, 1964b, a); however, alkali addition cannot be recommended for manual TIC sampling (Laporte-Urbe, 2019). Nevertheless, the good agreement between the **calculated HCO_3^-** and TIC values, as well as between the **calculated** and **continuous dCO_2** values (Table 1), highlights the suitability of the ATR-IR technique and sensor for continuously monitoring CO_2 holdup and dCO_2 concentrations.

The results also support, as a discrete sampling alternative, to target ruminal HCO_3^- using the protocols described by Hille et al. (2016), in conjunction with *in situ* pH measurements, to indirectly estimate ruminal dCO_2 using the equations described here (Eq 1).

Parameter	Dietsxrun	Nxn	Mean	SD	SEM	Percentile			Normality	Skewness	Kurtosis
						10	50	90			
pH	Low-peNDF 1 st run	3x45	6.08	0.219	0.033	5.75	6.07	6.41	0.47	0.15	-0.36
	High-RDS 2 nd run	3x45	6.31	0.349	0.052	5.76	6.41	6.72	0.01	-0.54	-0.83
	Combined 3 rd run	3x45	6.22	0.193	0.029	6.01	6.24	6.46	0.25	-0.69	1.60
TIC, mM	Low-peNDF 1 st run	3x43	28.9	8.19	1.25	19.1	27.3	40.6	0.04	0.79	0.41
	High-RDS 2 nd run	3x45	33.6	12.44	1.85	20.8	31.4	54.1	0.03	0.47	-0.83
	Combined 3 rd run	3x45	27.4	6.30	0.94	20.3	25.7	36.3	0.45	0.42	-0.18
observed dCO ₂ , mM	Low-peNDF 1 st run	3x43	17.9	4.33	0.66	12.8	17.2	22.4	0.01	1.22	2.42
	High-RDS 2 nd run	3x45	15.6	3.72	0.55	11.1	15.2	19.2	0.01	1.02	2.44
	Combined 3 rd run	3x45	15.3	2.93	0.44	10.6	15.8	18.9	0.54	-0.38	-0.24
calculated dCO ₂ , mM	Low-peNDF 1 st run	3x43	55.2	23.38	3.57	30.5	46.8	91.7	0.01	0.76	-0.44
	High-RDS 2 nd run	3x45	40.9	31.43	4.68	18.1	31.3	62.1	0.00	3.04	11.76
	Combined 3 rd run	3x45	38.7	16.50	2.46	22.0	37.4	57.2	0.00	1.97	6.74

Parameter	Dietsxrun	Nxn	Mean	SD	SEM	Percentile			Normality	Skewness	Kurtosis
						10	50	90			
continuous pH	Low-peNDF 1 st run	3x51,368	5.77	0.293	0.001	5.37	5.78	6.16	-	- 0.17	- 0.56
	High-RDS 2 nd run	3x51,212	5.91	0.433	0.002	5.36	5.86	6.53	-	0.33	- 0.64
	Combined 3 rd run	3x51,092	5.65	0.305	0.001	5.25	5.63	6.07	-	0.16	- 0.81
continuous dCO ₂ , mM	Low-peNDF 1 st run	1x25,511	74.7	12.38	0.08	58.1	75.7	88.7	-	- 0.26	1.38
	High-RDS 2 nd run	1x25,929	73.0	12.64	0.08	58.2	71.8	90.5	-	0.08	0.21
	Combined 3 rd run	1x25,474	59.1	14.86	0.09	39.9	59.4	77.7	-	0.37	1.18
calculated HCO ₃ ⁻ , mM	Low-peNDF 1 st run	1x1440	20.6	6.05	0.16	12.8	20.3	27.7	-	0.47	-0.29
	High-RDS 2 nd run	1x1440	28.0	12.03	0.32	17.9	23.6	49.2	-	1.51	1.30
	Combined 3 rd run	1x1440	12.0	2.89	0.08	8.8	11.4	16.4	-	0.80	-0.06

Table 1. Descriptive statistics of ruminal parameters measured by manual and continuous sampling methods (see the document for details).

The diets were low physically effective neutral detergent fibre (Low-peNDF) in the 1st run, high ruminally degradable starch (High-RDS) in the 2nd run, and a combination of both previous diets (Combined) in the 3rd run. Cattle (N) and records/samples (n). Manual sampling of ruminal pH (pH) and total inorganic carbon (TIC).

Continuous ruminal pH (continuous pH) and dCO_2 concentration (continuous dCO_2) measurements. The Observed dCO_2 was calculated with Eq 1. The dCO_2 derived from TIC (calculated dCO_2) and the HCO_3^- derived from the pH and dCO_2 sensor (calculated HCO_3^-) were computed using Eq 2. The median (50th percentile) and the 10th and 90th percentiles, respectively. Normality of discrete manual samples was assessed using the Shapiro-Wilk test ($p = 0.05$). For continuous measurements, descriptive statistics provide a reliable assessment of normality due to the Central Limit Theorem.

Continuous ruminal dCO_2 monitoring. The law of large numbers justified the reliance on descriptive statistics for analysing the continuous sensor data rather than solely statistical comparisons (Table 1). Multiple independent measurements of a physiological phenomenon typically follow a normal distribution, and the central value tends to be closer to the expected mean value, the Central Limit Theorem (Van der Vaart, 2000). The agreement between discrete measurements of pH, **calculated dCO_2** , and **TIC** by manual sampling, and continuous measurements of pH, dCO_2 , and **calculated HCO_3^-** , respectively (Table 1), suggests a high likelihood that all parameters originated from the same population. The small kurtosis, skewness, and similar central values, both mean and median, for all diets indicated that the continuous dCO_2 and pH recordings conformed to a Gaussian curve (Figure 1 and Table 1). The normal distribution of these biological parameters justified normalisation for detecting disease, comparing diets, and eliminating drift or calibration errors (Nocek et al., 2002; AlZahal et al., 2007a; Villot et al., 2018). Consequently, the goodness of fit of the output of the sensors employed in this study suggest that they accurately detected ruminal pH and dCO_2 within the physiological and pathological range (Figure 1 and Table 1), supporting the first hypothesis that ATR-IR is well-suited for continuous ruminal dCO_2 monitoring.

The range of ruminal dCO_2 concentrations detected by ATR-IR was 0 to 130 mM (Table 1). These results were comparable to the values for ruminal dCO_2 described for sheep (Chou and Walker, 1964b, a). The average ruminal dCO_2 values for the Low-peNDF, High- RDS, and Combined diets were 74.7, 73.0, and 59.1 mM, respectively (Table 1). These values were similar to those described for intact cattle (69.7 mM) and fistulated cattle (43.6 mM) and to the theoretical average ruminal dCO_2 of ~60 mM (Kohn and Dunlap, 1998; Wang et al., 2019). The observed peak ruminal dCO_2 values for the Low-peNDF (171 mM), Combined (151 mM), and High-RDS (117 mM) diets cannot be dismissed as biologically implausible. These findings challenge the previously proposed static view of the ruminal buffering system, and the saturation of the ruminal fluid at 60 mM of dCO_2 (Russell and Chow, 1993; Kohn and Dunlap, 1998).

To provide context, human blood dCO_2 rarely exceeds ~5% of the total CO_2 content, with venous dCO_2 levels at rest and during exercise being ~1.4 mM and ~2.4 mM, respectively (Geers and Gros, 2000). Cattle venous dCO_2 levels, calculated from total CO_2 using Equation 1, might range from 2.2 to 2.5 mM under SARA (Gianesella et al.,

2010). Further, $d\text{CO}_2$ concentrations at rest in the inner lining fluid of the alveolar region are ~ 1.3 mM, corresponding to a 5% end-tidal CO_2 gas content (Shao and Friedman, 2020). Ruminants exposed to over 5% CO_2 gas in metabolic chambers develop tachypnoea (Blaxter, 1962). Moreover, alveolar $d\text{CO}_2$ levels might exceed blood levels at $>10\%$ CO_2 gas exposure, reaching ~ 2.4 mM, which is considered toxic (Abolhassani et al., 2009). In contrast, ruminal $d\text{CO}_2$ values above 80 mM were routinely observed in all diets and were readily available for absorption (Table 1, Figure 2.2abc), these values are 30 times higher than blood.

The rapid equilibrium between ruminal and blood $d\text{CO}_2$ pools is well established (Whitelaw et al., 1972; Veenhuizen et al., 1988) primarily due to CO_2 diffusion (Endeward et al., 2017; Arias-Hidalgo et al., 2018) and the utilization of ruminal CO_2 for SCFA absorption (Ash and Dobson, 1963; Rackwitz and Gabel, 2018). These exceptionally high ruminal $d\text{CO}_2$ concentrations suggest that ruminants are constantly exposed to hypoxemic/hypercapnic conditions, which explains several known unique physiological adaptations, such as the high ruminal epithelial cholesterol content (Steele et al., 2011; Jiang and Loor, 2023) which limits CO_2 diffusion (Arias-Hidalgo et al., 2018), the low oxygen affinity of adult ruminant haemoglobin (Bunn, 1980) which improves peripheral tissues oxygenation, and the enhanced blood HCO_3^- carrying capacity due to the chloride shift (Westen and Prange, 2003), blood CO_2 is carried mainly as HCO_3^- (Geers and Gros, 2000). Nevertheless, the development of CO_2 holdup might enhance CO_2 absorption and overwhelm the cellular buffering system, as the capacity to eliminate this CO_2 excess is impaired and $d\text{CO}_2$ is a readily available source for absorption. Moreover, CO_2 poisoning triggers a strong inflammatory response in the lungs (Liu et al., 2008; Abolhassani et al., 2009) similar to the inflammation commonly reported during SARA onset (Penner et al., 2011). Therefore, if we can confirm that critical $d\text{CO}_2$ concentrations are sustained for extended time periods or CO_2 holdup, we could suspect that CO_2 poisoning is triggering SARA.

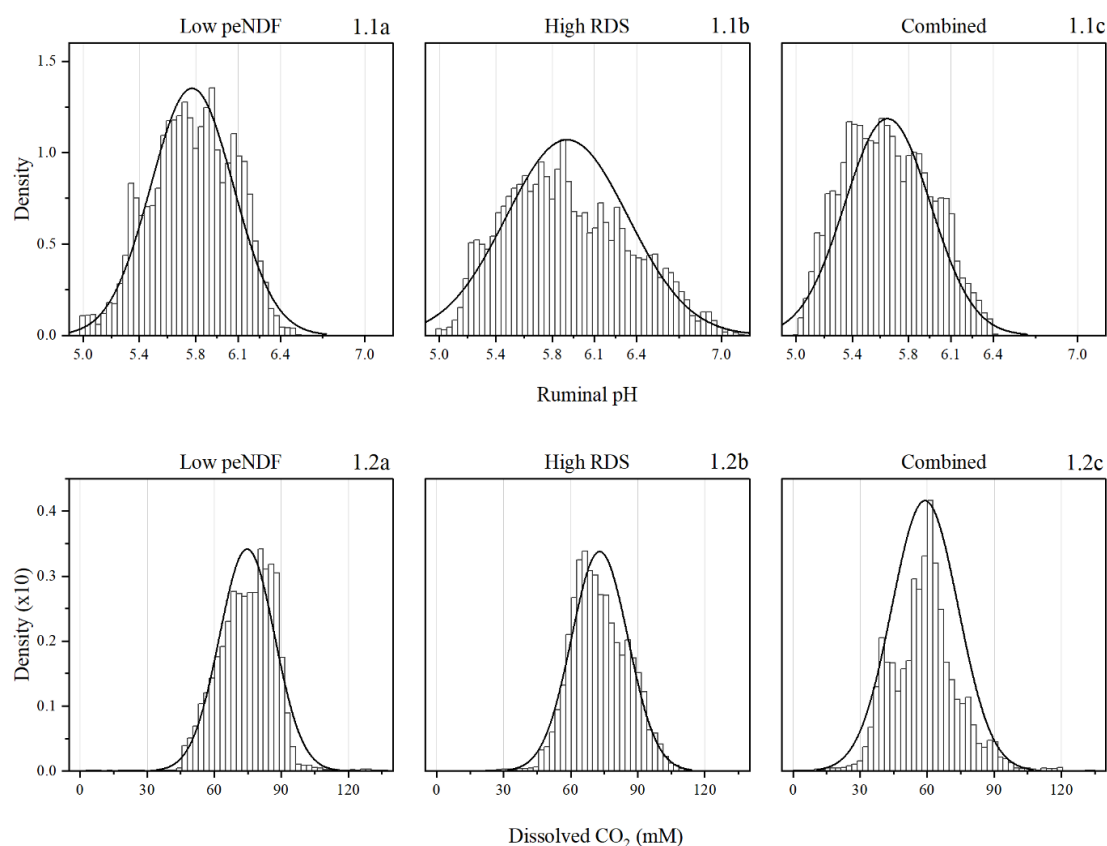


Fig. 1. Histograms and normal curve fits for continuous measurements of ruminal pH and dissolved CO₂ concentrations (mM) are shown for lactating dairy cattle fed three diets in consecutive periods: Low-peNDF (low physically effective neutral detergent fiber, 1.1a and 1.2a), High-RDS (high ruminally degradable starch, 1.1b and 1.2b), and Combined (1.1c and 1.2c).

Ruminal pH cannot predict dCO₂ concentrations. In all the diets, High or Critical dCO₂ levels were consistently observed postprandially, which were paralleled by a decline in ruminal pH (Figure 2.2a-c). This phenomenon was attributed to the interconversion of HCO₃⁻ to dCO₂ during H₃O⁺ buffering (Laporte-Urbe, 2016). Nevertheless, pH is ultimately a quotient, limiting its ability to directly measure the specific concentrations of individual components; for instance, two HCO₃⁻/dCO₂ solutions with the same pH (100/100 mM and 10/10 mM) exhibit distinct concentrations (Eq 2). Feeding the combined diet resulted in the lowest pH (Fig 1.1c) and minimum dCO₂ (Fig 1.2c), whereas the high-RDS diet produced the highest pH (Fig 1.1b) and maximum dCO₂ (Fig 1.2b), corroborating the statement. The reduced pH in the Combined diet can be attributable not only to lower dCO₂ but also to decreased HCO₃⁻ levels. Conversely, both HCO₃⁻ and dCO₂ concentrations were high in the High-RDS diet, bringing the pH closer to the equilibrium constant for CO₂ (pK_{a1} ≈ 6.1). The distinctive

feature of CO_2 holdup is that both ruminal dCO_2 and HCO_3^- concentrations were elevated. Therefore, CO_2 holdup explains why low ruminal pH does not always predict clinical SARA onset (Villot et al., 2018) or that SARA affected cattle present larger variation in ruminal pH than healthy cattle (Nocek et al., 2002; Penner et al., 2007; Dohme et al., 2008). The equilibrium between CO_2 species dictates the pH of the solution, if both molecules are in high concentrations the ruminal pH might seem normal (Eq 2), even when critical dCO_2 might be present. Therefore, while high dCO_2 can coexist with low pH, it is only during CO_2 holdup that critical dCO_2 concentrations persist for prolonged postprandial periods, a condition that cannot be accurately predicted by the ruminal pH scale but can be effectively monitored by the ATR-IR technique.

	Dietsxrun		
	Low-peNDF 1 st run	High-RDS 2 nd run	Combined 3 rd run
Performance parameters, kg/d			
N	12	12	9
DMI	24.7 ± 0.85 ^a	18.4 ± 0.85 ^b	24.7 ± 0.98 ^a
MY	36.1 ± 0.48 ^a	32.8 ± 0.48 ^b	33.2 ± 0.56 ^b
ECM	37.2 ± 0.51 ^a	34.6 ± 0.51 ^b	35.6 ± 0.59 ^a
Milk component yield, kg/d			
Fat	1.37 ± 0.02 ^a	1.27 ± 0.02 ^b	1.33 ± 0.02 ^{ab}
Protein	1.22 ± 0.02 ^a	1.15 ± 0.02 ^b	1.18 ± 0.02 ^{ab}
Lactose	1.62 ± 0.02 ^a	1.49 ± 0.02 ^b	1.48 ± 0.03 ^b
Ventral ruminal sac parameters			
N	45	45	45
Acetate, mM	58.7 ± 0.29 ^a	55.8 ± 0.29 ^b	56.6 ± 0.29 ^b
Propionate, mM	29.3 ± 0.29 ^a	33.9 ± 0.29 ^b	32.6 ± 0.29 ^c
Butyrate, mM	11.7a ± 0.11 ^a	8.9 ± 0.11 ^b	9.9 ± 0.11 ^c
A/P ratio	2.01 ± 0.028 ^a	1.67 ± 0.028 ^b	1.79 ± 0.028 ^c
Total SCFAs, mM	114.6 ± 2.46 ^a	125.5 ± 2.46 ^b	114.9 ± 2.46 ^a
Lactate, µM, n=27	9.2 ± 1.72	21.2 ± 2.21	41.1 ± 7.91
Viscosity, mPa.S	2.1 ± 0.18 ^a	3.6 ± 0.18 ^b	4.4 ± 0.18 ^c
Surface Tension, mN/m	67.2 ± 0.50 ^a	70.5 ± 0.5 ^b	71.5 ± 0.5 ^b

Table 2. Summary of longitudinal trial results in fistulated cattle. Mean (±SEM) values for performance, milk components, and ruminal parameters across three runs with three fistulated cattle fed three diets. This table consolidates findings described in the previous report of this experiment (Laporte-Urbe, 2019).

The diets were low physically effective neutral detergent fibre (Low-peNDF) in the 1st run, high ruminally degradable starch (High-RDS) in the 2nd run and the combination of both previous diets (Combined) in the 3rd run. Dry matter intake (DMI), milk yield (MY), short-chain fatty acids (SCFAs) and the ruminal acetate to propionate ratio (A/P ratio). The energy corrected MY (ECM) = milk NEL output (Mcal/d)/0.7 Mcal of NEL/kg of milk, were milk NEL output (Mcal/d) = milk yield, kg/d \times (0.0929 \times milk fat % + 0.0563 \times milk protein % + 0.0395 \times milk lactose %). All comparison were made at the 95% confidence level ($P < 0.05$) and means that do not share a letter are significantly different (Bonferroni).

The positive effect of high ruminal dCO₂. Ruminal CO₂ species play a pivotal role epithelial metabolism. The majority of the intracellular HCO₃⁻ and H₃O⁺ available for SCFA⁻ and Na⁺ exchange (Penner et al., 2011; Rabbani et al., 2021) are likely derived from ruminal dCO₂ (Veenhuizen et al., 1988; Rackwitz and Gabel, 2018), which is most likely absorbed into the epithelial cell with H₂O through aquaporins (Endeward et al., 2017). Aquaporins are abundantly expressed in the ruminal epithelia (Zhong et al., 2020). Therefore, high ruminal dCO₂ increases epithelial H₂O absorption (Dobson et al., 1970) and carbonic anhydrase bound to the intracellular aquaporin domains (Vilas et al., 2015; Rabbani et al., 2021) may expedite intracellular CO₂ hydration, leading to the formation of HCO₃⁻ and H₃O⁺, which in turn enhances SCFA⁻ uptake (Ash and Dobson, 1963; Gabel et al., 1991; Rackwitz and Gabel, 2018). The rehydration by ruminal carbon anhydrase of the secreted intracellular HCO₃⁻ and H₃O⁺ into dCO₂ provides the perfect (re) cycling system for nutrient uptake and explains the widespread expression of carbon anhydrase throughout the gastrointestinal tract (Carter and Parsons, 1971; Mau and Südekum, 2011).

The effect of high ruminal dCO₂ concentrations in this experiment confirm that CO₂ hydration plays a crucial role in nutrient uptake. For instance, cattle fed the Low-peNDF diet produced more milk (ECM, 37.2 vs. 35.6 kg/day) and lactose (1.62 vs. 1.48 kg/day) than cattle fed the Combined diet at a similar feed intake of 24.7 kg/day (Table 2). The diets were specifically formulated to provide similar amounts of energy and protein, and no significant differences in productivity were expected (Laporte-Urbe, 2019). The rumen AUC maps for the Low-peNDF diet revealed a balanced pH (Figure 2.1a) and consistently high dCO₂ levels (Figure 2.2a) throughout the day. In contrast, cattle fed the Combined diet exhibited lower dCO₂ levels (Figure 2.2c) and a more acidic ruminal pH (Figure 2.1c). The lower ruminal pH in the Combined diet might indicate greater availability of SCFA, as they are passively absorbed as acids (Dijkstra et al., 1993; Penner et al., 2011). However, feeding the Combined diet did not result in a higher milk yield when compared with the Low-peNDF diet (Table 2). In fact, the reduced ruminal propionate levels with the Low-peNDF diet suggested enhanced SCFA absorption, as supported by a time series of propionate, see Laporte-Urbe (2019). Propionate absorption leads to glucose formation, which

boosts lactose production and milk yield from the mammary gland (Aschenbach et al., 2010; Penner et al., 2011). Consequently, the higher milk and lactose yields with the Low-peNDF diet can be attributed to increased ruminal propionate absorption (Table 2), which was likely promoted by the high dCO₂ levels observed in the rumen AUC map (Figure 2.2a), confirming the positive effect of high dCO₂ on ruminal absorption (Ash and Dobson, 1963; Gabel et al., 1991).

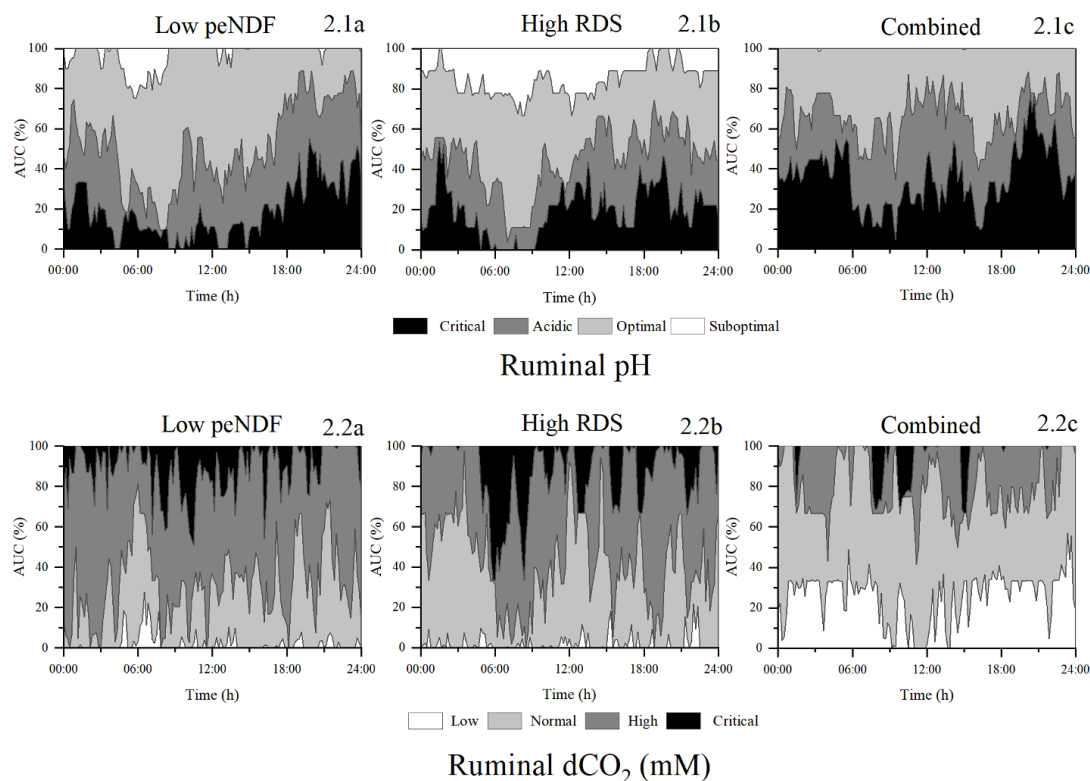


Fig. 2. Rumen maps depicting the most frequent category (area under the curve, AUC, %) of ruminal pH (2.1a-c) and dissolved CO₂ (dCO₂, 2.2a-c) in lactating dairy cattle fed three diets: low physically effective neutral detergent fiber (Low-peNDF; 2.1a and 2.2a), high ruminally degradable starch (High-RDS; 2.1b and 2.2b), and a combination of both (Combined; 2.1c and 2.2c). The category descriptions are provided within the text.

CO₂ holdup might lead to clinical SARA signs. The ruminal AUC map for pH (Figure 2.1b) indicated that cattle had the lowest SARA risk when fed the High-RDS diet based on the conventional definition of SARA based on the pH scale (Nocek et al., 2002; Villot et al., 2018). However, cattle consuming the High-RDS diet exhibited typical SARA symptoms: reduced feed intake and milk yield, Table 2 (Nocek et al., 2002; Dohme et al., 2008). The rumen AUC map revealed that cattle fed the High-RDS diet experienced critical dCO₂ concentrations for extended postprandial periods, or CO₂ holdup (Spikes of critical values in Figure 2.2b). The high ruminal SCFA

levels and the lower milk yield suggested impaired activity of the sodium–hydrogen exchanger (NHE) with the High-RDS diet (Penner et al., 2011; Zhao et al., 2017). Otherwise, high ruminal SCFA production and undisturbed absorption should increase milk yield, besides low feed intake with High-RDS should reduce SCFA production and not enhance it, Table 2 (Dijkstra et al., 1993).

Under normal conditions, NHE regulates intracellular H_3O^+ exchange with ruminal Na^+ (Penner et al., 2011; Zhao et al., 2017). Since the ruminal epithelium is H_3O^+ -impermeable, the intracellular H_3O^+ must originate from either ruminal CO_2 hydration or intracellular SCFA metabolism (Penner et al., 2011; Rackwitz and Gabel, 2018). CO_2 holdup can lead to ruminal hyperosmolarity, which diminishes feed intake, H_2O absorption, and Na^+ absorption and is linked to the onset of SARA (Dobson et al., 1970; Lodemann and Martens, 2006; Steele et al., 2011). The impaired H_2O absorption resulting from hyperosmolarity, could potentially reduce intracellular H_3O^+ formation and NHE activity, thereby impairing SCFA absorption. This could explain the elevated ruminal SCFA concentrations observed in cattle fed the High-RDS diet and during SARA (Penner et al., 2011).

Notably, the epithelial response to SARA involves increased intracellular SCFA metabolism and enhanced NHE expression (Zhao et al., 2017), which might bolster intracellular H_3O^+ and HCO_3^- formation and SCFA absorption. Additionally, intracellular cholesterol synthesis and deposition are intensified (Steele et al., 2011; Zhao et al., 2017), likely as a response to high dCO_2 exposure and to reduce dCO_2 diffusion (Arias-Hidalgo et al., 2018). Therefore, clinical SARA symptoms may come from CO_2 holdup development, as depicted by the rumen AUC maps. Prolonged exposure to these critical dCO_2 conditions might elevate the risk of SARA or CO_2 poisoning.

Ruminal CO_2 holdup monitoring. The “rumen AUC maps” depict the daily ruminal fermentation pattern associated with ruminal dCO_2 and influenced by dietary components, daily feed intake, feed allowance and management routines (Gibbs and Laporte Uribe, 2009). Therefore, these maps enable the monitoring of ruminal dCO_2 by classifying it into categories with biological significance. The dCO_2 detected by ATR-IR sensor at these selected thresholds aligned with the established biological effect of CO_2 . For instance, ruminal bacterial growth starts at 12 to 20 mM dCO_2 (Dehority, 1971), and the optimal succinate production, the primary ruminal propionate precursor, requires a greater than the ruminal average, > 60 mM (Dehority, 1971; Samuelov et al., 1991). A ruminal dCO_2 threshold over 80 mM might signal an increased risk of hyperosmolarity (Lodemann and Martens, 2006; Steele et al., 2011), impaired buffering capacity (Turner and Hodgetts, 1955; Hille et al., 2016) and/or an increased risk of epithelial CO_2 poisoning (Liu et al., 2008). Additionally, feeding consistent diets and adhering to stable feeding management routines enhance feed intake, milk yield, and lower the risk of nutritional disorders (Deming et al., 2013; Sova et al., 2013). Consequently, rumen AUC maps provide valuable insight on the health and productivity of dairy cattle subjected to diverse diets and management practices.

Furthermore, the (cross) tabulation of frequencies on daily “contingency tables” with the proposed categorical analysis streamlines the statistical comparison of ruminal patterns, i.e., the 144-time segment and 4-category matrix can be analysed utilising the Pearson chi-square (X^2), G-test or Bayesian inference (Van der Vaart, 2000). Consequently, rumen AUC maps establish the foundation for “precision ruminal fermentation”: the selection of diets and management practices that optimise ruminal fermentation, reduce waste products and prevent nutritional diseases associated to SARA by continuously measuring dCO₂ concentrations and CO₂ holdup formation.

Conclusions

Dissolved CO₂ is ubiquitous in the rumen environment, present in substantial and varied amounts. For the first time ruminal dCO₂ presence and dynamics including CO₂ holdup have been described *in situ*. Optimal rumen function relies heavily on dCO₂ concentrations, as key component of the ruminal buffering system. This crucial contribution has gone largely unrecognized. Conversely, disruption of the ruminal buffering system, leading to CO₂ holdup, could potentially heighten the risk of CO₂ poisoning and trigger clinical SARA signs. These results warrant further investigation. I highlight a novel methodology to validate or refute this hypothesis.

Statements and Declarations

Acknowledgements

This study was supported and financed by GEA Farm Technologies GmbH. I am deeply indebted to Wageningen University, particularly the team at Dairy Campus, Leeuwarden, especially Dr. R. Goselink, Wageningen Livestock Research, for their indispensable contribution to establishing, implementing, and carrying out the experimental work and sample analysis. I extend my heartfelt gratitude to Dr. P. Brueckner, Miss A. Angopian, and Mr. M. Weidlich for their invaluable professional support throughout this project.

Author contributions

JLU designed the study, performed the experiment, analysed the data, and wrote this manuscript.

Competing interests

The author is the inventor of the indwelling ruminal sensors. This research provides partial justification for the use of these systems for disease prevention and improved sustainability.

Data availability

Due to ethical and privacy considerations, the data that support this study cannot be publicly shared. However, upon reasonable request to the corresponding author, access to the data may be granted when appropriate.

Additional information

Correspondence and requests for materials should be addressed to joselaporte@hotmail.com

References

- Abolhassani, M., A. Guais, P. Chaumet-Riffaud, A. J. Sasco, and L. Schwartz. 2009. Carbon dioxide inhalation causes pulmonary inflammation. *Am. J. Physiol. Lung Cell. Mol. Physiol.* 296(4):L657-L665.
- AlZahal, O., E. Kebreab, J. France, and B. W. McBride. 2007a. A mathematical approach to predicting biological values from ruminal pH measurements. *J. Dairy Sci.* 90(8):3777-3785. doi: 10.3168/jds.2006-534
- AlZahal, O., B. Rustomo, N. E. Odongo, T. F. Duffield, and B. W. McBride. 2007b. Technical note: A system for continuous recording of ruminal pH in cattle. *J. Anim. Sci.* 85(1):213-217. doi: 10.2527/jas.2006-095
- Arias-Hidalgo, M., S. Al-Samir, G. Gros, and V. Endeward. 2018. Cholesterol is the main regulator of the carbon dioxide permeability of biological membranes. *Am. J. Physiol. Cell Physiol.* 315(2):C137-C140. doi: 10.1152/ajpcell.00139.2018
- Aschenbach, J. R., N. B. Kristensen, S. S. Donkin, H. M. Hammon, and G. B. Penner. 2010. Gluconeogenesis in dairy cows: the secret of making sweet milk from sour dough. *IUBMB Life* 62(12):869-877. doi: 10.1002/iub.400
- Ash, R. W., and A. Dobson. 1963. The effect of absorption on the acidity of rumen contents. *Journal of Physiology* 169(1):39-61. doi: 10.1113/jphysiol.1963.sp007240
- Blaxter, K. L. 1962. The Energy metabolism of Ruminants. Hutchison & CO. LTD.
- Buchholz, J., M. Graf, B. Blombach, and R. Takors. 2014. Improving the carbon balance of fermentations by total carbon analyses. *Biochem. Eng. J.* 90:162-169.
- Bunn, H. F. 1980. Regulation of hemoglobin function in mammals. *Am. Zool.* 20(1):199-211.
- Carter, M. J., and D. S. Parsons. 1971. The isoenzymes of carbonic anhydrase: tissue, subcellular distribution and functional significance, with particular reference to the intestinal tract. *Journal of Physiology* 215(1):71-94.
- Chou, K. C., and D. M. Walker. 1964a. The effect on the rumen composition of feeding sheep diets supplying different starches. I. The variation in rumen composition of sheep fed lucerne or wheat as the sole diet. *J. Agric. Sci.* 62(01):7-13.

- Chou, K. C., and D. M. Walker. 1964b. The effect on the rumen composition of feeding sheep diets supplying different starches. II. The partition of nitrogen, pH, volatile fatty acids, protozoal numbers, enzymic activity and certain other chemical constituents. *J. Agric. Sci.* 62(01):15-25.
- De Veth, M. J., and E. S. Kolver. 2001. Diurnal variation in pH reduces digestion and synthesis of microbial protein when pasture is fermented in continuous culture. *J. Dairy Sci.* 84(9):2066-2072.
- Dehority, B. A. 1971. Carbon dioxide requirement of various species of rumen bacteria. *J. Bacteriol.* 105(1):70-76.
- Deming, J. A., R. Bergeron, K. E. Leslie, and T. J. DeVries. 2013. Associations of housing, management, milking activity, and standing and lying behavior of dairy cows milked in automatic systems. *J. Dairy Sci.* 96(1):344-351. doi: 10.3168/jds.2012-5985
- Dijkstra, J., H. Boer, J. Van Bruchem, M. Bruining, and S. Tamminga. 1993. Absorption of volatile fatty acids from the rumen of lactating dairy cows as influenced by volatile fatty acid concentration, pH and rumen liquid volume. *Br. J. Nutr.* 69(02):385-396.
- Dijkstra, J., J. L. Ellis, E. Kebreab, A. B. Strathe, S. López, J. France, and A. Bannink. 2012. Ruminant pH regulation and nutritional consequences of low pH. *Anim. Feed Sci. Technol.* 172(1-2):22-33. doi: 10.1016/j.anifeedsci.2011.12.005
- Dobson, A., A. F. Sellers, and G. T. Shaw. 1970. Absorption of water from isolated ventral sac of rumen of the cow. *J. Appl. Physiol.* 28(1):100-104. doi: 10.1152/jappl.1970.28.1.100
- Dohme, F., T. J. DeVries, and K. A. Beauchemin. 2008. Repeated ruminal acidosis challenges in lactating dairy cows at high and low risk for developing acidosis: ruminal pH. *J. Dairy Sci.* 91(9):3554-3567. (Research Support, Non-U.S. Gov't) doi: 10.3168/jds.2008-1264
- Duffield, T., J. C. Plaizier, A. Fairfield, R. Bagg, G. Vessie, P. Dick, J. Wilson, J. Aramini, and B. W. McBride. 2004. Comparison of techniques for measurement of rumen pH in lactating dairy cows. *J. Dairy Sci.* 87(1):59-66.
- Endeward, V., M. Arias-Hidalgo, S. Al-Samir, and G. Gros. 2017. CO(2) Permeability of Biological Membranes and Role of CO(2) Channels. *Membranes (Basel)* 7(4) doi: 10.3390/membranes7040061
- Gabel, G., S. Vogler, and H. Martens. 1991. Short-chain fatty acids and CO₂ as regulators of Na⁺ and Cl⁻ absorption in isolated sheep rumen mucosa. *J Comp Physiol B* 161(4):419-426. doi: 10.1007/bf00260803
- GebSKI, M., and R. K. Wong. 2007. An Efficient Histogram Method for Outlier Detection. 4443:176-187. doi: 10.1007/978-3-540-71703-4_17
- Geers, C., and G. Gros. 2000. Carbon dioxide transport and carbonic anhydrase in blood and muscle. *Physiol. Rev.* 80(2):681-715. doi: 10.1152/physrev.2000.80.2.681
- Ganesella, M., M. Morgante, C. Cannizzo, A. Stefani, P. Dalvit, V. Messina, and E. Giudice. 2010. Subacute ruminal acidosis and evaluation of blood gas analysis in dairy cow. *Vet. Med. Int.* 2010:1-4. doi:

- Gibbs, S. J., and J. Laporte Uribe. 2009. Diurnal patterns of rumen pH and function in dairy cows on high quality temperate pastures of the South Island of New Zealand. *J. Dairy Sci.* 92(E-Suppl. 1):585.
- Hille, K. T., S. K. Hetz, J. Rosendahl, H. S. Braun, R. Pieper, and F. Stumpff. 2016. Determination of Henry's constant, the dissociation constant, and the buffer capacity of the bicarbonate system in ruminal fluid. *J. Dairy Sci.* 99(1):369–385. doi: 10.3168/jds.2015–9486
- Jiang, Q., and J. J. Loor. 2023. The Lipidome of the Gastrointestinal Tract in Lactating Holstein Cows. *Ruminants* 3(1):76–91. doi: 10.3390/ruminants3010007
- Kohn, R. A., and T. F. Dunlap. 1998. Calculation of the buffering capacity of bicarbonate in the rumen and in vitro. *J. Anim. Sci.* 76(6):1702–1709.
- Laporte-Uribe, J. A. 2016. The role of dissolved carbon dioxide in both the decline in rumen pH and nutritional diseases in ruminants. *Anim. Feed Sci. Technol.* 219:268–279. doi: 10.1016/j.anifeedsci.2016.06.026
- Laporte-Uribe, J. A. 2019. Rumen CO₂ species equilibrium might influence performance and be a factor in the pathogenesis of subacute ruminal acidosis. *Translational Animal Science* 3(4):1081–1098. doi: 10.1093/tas/txz144
- Liu, Y., B. K. Chacko, A. Ricksecker, R. Shingarev, E. Andrews, R. P. Patel, and J. D. Lang Jr. 2008. Modulatory effects of hypercapnia on in vitro and in vivo pulmonary endothelial-neutrophil adhesive responses during inflammation. *Cytokine* 44(1):108–117. doi: 10.1016/j.cyto.2008.06.016
- Lodemann, U., and H. Martens. 2006. Effects of diet and osmotic pressure on Na⁺ transport and tissue conductance of sheep isolated rumen epithelium. *Exp. Physiol.* 91(3):539–550. doi: 10.1113/expphysiol.2005.032078
- Mau, M., and K.-H. Südekum. 2011. Secretory carbonic anhydrase II – Finding the evolutionary key to the symbiosis of animal hosts and their cellulose-fermenting bacteria. *Hypothesis* 9(1):E1–6.
- Nocek, J. E., J. G. Allman, and W. P. Kautz. 2002. Evaluation of an indwelling ruminal probe methodology and effect of grain level on diurnal pH variation in dairy cattle. *J. Dairy Sci.* 85(2):422–428.
- Penner, G. B., K. A. Beauchemin, and T. Mutsvangwa. 2007. Severity of ruminal acidosis in primiparous holstein cows during the periparturient period. *J. Dairy Sci.* 90(1):365–375. doi: 10.3168/jds.S0022-0302(07)72638-3
- Penner, G. B., M. A. Steele, J. R. Aschenbach, and B. W. McBride. 2011. Ruminant Nutrition Symposium: Molecular adaptation of ruminal epithelia to highly fermentable diets. *J. Anim. Sci.* 89(4):1108–1119. doi: 10.2527/jas.2010–3378
- Rabbani, I., H. Rehman, H. Martens, K. A. Majeed, M. S. Yousaf, and Z. U. Rehman. 2021. Carbonic anhydrase influences asymmetric sodium and acetate transport across omasum of sheep. *Anim Biosci* 34(5):880–885.

doi: 10.5713/ajas.20.0163

- Rackwitz, R., and G. Gabel. 2018. Effects of dissolved carbon dioxide on the integrity of the rumen epithelium: An agent in the development of ruminal acidosis. *J Anim Physiol Anim Nutr (Berl)* 102(1):e345-e352. doi: 10.1111/jpn.12752
- Russell, J. B. 1998. The Importance of pH in the Regulation of Ruminal Acetate to Propionate Ratio and Methane Production In Vitro. *J. Dairy Sci.* 81(12):3222-3230. doi: [https://doi.org/10.3168/jds.S0022-0302\(98\)75886-2](https://doi.org/10.3168/jds.S0022-0302(98)75886-2)
- Russell, J. B., and J. M. Chow. 1993. Another theory for the action of ruminal buffer salts: decreased starch fermentation and propionate production. *J. Dairy Sci.* 76(3):826-830.
- Samuelov, N. S., R. Lamed, S. Lowe, and J. G. Zeikus. 1991. Influence of CO₂-HCO₃⁻ levels and pH on growth, succinate production, and enzyme activities of *Anaerobiospirillum succiniciproducens*. *Appl. Environ. Microbiol.* 57(10):3013-3019.
- Schädle, T., B. Pejčic, and B. Mizaikoff. 2016. Monitoring dissolved carbon dioxide and methane in brine environments at high pressure using IR-ATR spectroscopy. *Analytical Methods* 8(4):756-762.
- Shao, X. M., and T. C. Friedman. 2020. Last Word on Viewpoint: pH Buffer capacity and pharmacokinetics: two remaining questions. *J Appl Physiol* (1985) 128(4):1063-1064. doi: 10.1152/japplphysiol.00165.2020
- Sova, A. D., S. J. Leblanc, B. W. McBride, and T. J. Devries. 2013. Associations between herd-level feeding management practices, feed sorting, and milk production in freestall dairy farms. *J. Dairy Sci.* 96(7):4759-4770. doi: 10.3168/jds.2013-6679
- Steele, M. A., G. Vandervoort, O. AlZahal, S. E. Hook, J. C. Matthews, and B. W. McBride. 2011. Rumen epithelial adaptation to high-grain diets involves the coordinated regulation of genes involved in cholesterol homeostasis. *Physiol. Genomics* 43(6):308-316. doi: 10.1152/physiolgenomics.00117.2010
- Turner, A. W., and V. E. Hodgetts. 1955. Buffer systems in the rumen of sheep. I. pH and bicarbonate concentration in relationship to pCO₂. *Crop Pasture Sci.* 6(1):115-124.
- Van der Vaart, A. W. 2000. Asymptotic statistics. Cambridge University Press, NY, USA.
- Veenhuizen, J. J., R. W. Russell, and J. W. Young. 1988. Kinetics of metabolism of glucose, propionate and CO₂ in steers as affected by injecting phlorizin and feeding propionate. *J. Nutr.* 118(11):1366-1375.
- Vilas, G., D. Krishnan, S. K. Loganathan, D. Malhotra, L. Liu, M. R. Beggs, P. Gena, G. Calamita, M. Jung, R. Zimmermann, G. Tamma, J. R. Casey, and R. T. Alexander. 2015. Increased water flux induced by an aquaporin-1/carbonic anhydrase II interaction. *Mol. Biol. Cell* 26(6):1106-1118. doi: 10.1091/mbc.E14-03-0812
- Villot, C., B. Meunier, J. Bodin, C. Martin, and M. Silberberg. 2018. Relative reticulo-rumen pH indicators for subacute ruminal acidosis detection in dairy cows. *Animal* 12(3):481-490. doi: 10.1017/S1751731117001677

- Wang, R., M. Wang, X. M. Zhang, J. N. Wen, Z. Y. Ma, D. L. Long, J. P. Deng, and Z. L. Tan. 2019. Effects of rumen cannulation on dissolved gases and methanogen community in dairy cows. *J. Dairy Sci.* 102(3):2275–2282. doi: 10.3168/jds.2018-15187
- Westen, E. A., and H. D. Prange. 2003. A reexamination of the mechanisms underlying the arteriovenous chloride shift. *Physiol. Biochem. Zool.* 76(5):603–614.
- Whitelaw, F. G., J. M. Brockway, and R. S. Reid. 1972. Measurement of carbon dioxide production in sheep by isotope dilution. *Exp. Physiol.* 57(1):37–55.
- Wolin, M. J. 1960. A theoretical rumen fermentation balance. *J. Dairy Sci.* 43(10):1452–1459.
- Zhao, K., Y. H. Chen, G. B. Penner, M. Oba, and L. L. Guan. 2017. Transcriptome analysis of ruminal epithelia revealed potential regulatory mechanisms involved in host adaptation to gradual high fermentable dietary transition in beef cattle. *BMC Genomics* 18(1):976. doi: 10.1186/s12864-017-4317-y
- Zhong, C., A. Farrell, and G. S. Stewart. 2020. Localization of aquaporin-3 proteins in the bovine rumen. *J. Dairy Sci.* 103(3):2814–2820. doi: 10.3168/jds.2019-17735.

Declarations

Funding: GEA Farm Technologies provided the funding for this project.

Potential competing interests: I own patents related to dissolved Co2 monitoring.